

$\eta \rightarrow \pi^0 \gamma \gamma$ decay within a chiral unitary approach revisitedE. Oset,¹ J. R. Peláez,² and L. Roca³¹*Departamento de Física Teórica and IFIC, Centro Mixto Universidad de Valencia-CSIC, Institutos de Investigación de Paterna, Apartado 22085, 46071 Valencia, Spain*²*Departamento de Física Teórica II, Universidad Complutense, 28040 Madrid, Spain*³*Departamento de Física, Universidad de Murcia, E-30071, Murcia, Spain*

(Received 17 January 2008; published 7 April 2008)

In view of the recent experimental developments in the $\eta \rightarrow \pi^0 \gamma \gamma$ decay, and the fact that the Particle Data Group in the online edition of 2007 reports sizable changes of the radiative decay widths of vector mesons used as input in the theoretical calculations of E. Oset, J. R. Peláez, and L. Roca [Phys. Rev. D **67**, 073013 (2003)], a reevaluation of the decay width of the η in this channel has been done, reducing its uncertainty by almost a factor of 2. The new input of the Particle Data Group is used, and invariant mass distributions and total widths are compared with the most recent results from the AGS and MAMI experiments, and preliminary ones of KLOE. The agreement of the theory with the AGS and MAMI data is very good, both for the total rates and for the invariant mass distributions of the two photons.

DOI: [10.1103/PhysRevD.77.073001](https://doi.org/10.1103/PhysRevD.77.073001)

PACS numbers: 13.40.Hq, 12.39.Fe

I. INTRODUCTION

The $\eta \rightarrow \pi^0 \gamma \gamma$ reaction has been quite controversial given the large discrepancies between different theoretical approaches trying to match the scarce experimental data. For a long time the standard experimental results have been those of early experiments [1,2], giving $\Gamma = 0.84 \pm 0.18$ eV. More recent experiments with the Crystal Ball detector at AGS [3] reduced this value to $\Gamma = 0.45 \pm 0.12$ eV. A new reanalysis of AGS data gives $\Gamma = 0.285 \pm 0.031 \pm 0.049$ eV [4], and a more recent analysis with the Crystal Ball at MAMI provides the rate $\Gamma = 0.290 \pm 0.059 \pm 0.022$ eV [4]. At the same time the last two experiments have provided the much awaited invariant mass distribution for the two photons, which was thought to provide valuable information concerning the theoretical interpretation. Some preliminary results from KLOE at Frascati [5] are also available with values around $\Gamma = 0.109 \pm 0.035 \pm 0.018$ eV.

The theoretical models also show a similar dispersion of the results, from large values obtained using models with quark box diagrams [6,7] to much smaller ones, obtained mostly using ideas of chiral perturbation theory (ChPT), which are quoted in [8].

The $\eta \rightarrow \pi^0 \gamma \gamma$ reaction has been traditionally considered to be a borderline problem to test ChPT. The reason is that the tree-level amplitudes, both at $O(p^2)$ and $O(p^4)$, vanish. The first nonvanishing contribution comes at $O(p^4)$, either from loops involving kaons, largely suppressed due to the kaon masses, or from pion loops, again suppressed since they violate G parity and are thus proportional to $m_u - m_d$ [9]. The first sizable contribution comes at $O(p^6)$, but the coefficients involved are not precisely determined and one must rely upon models. In this sense, either vector meson dominance (VMD) [9–11], the Nambu-Jona-Lasinio model (NJL) [12], or the extended Nambu-Jona-Lasinio model (ENJL) [13,14] has been used

to determine these coefficients. However, the use of tree-level VMD to obtain the $O(p^6)$ chiral coefficients by expanding the vector meson propagators leads [9] to results about a factor of 2 smaller than the “all order” VMD term when one keeps the full vector meson propagator. The lesson obtained from these studies is that ChPT can be used as a guiding principle, but the strict chiral counting has to be abandoned since the $O(p^6)$ and higher orders involved in the full (“all order”) VMD results are larger than those of $O(p^4)$. Also, these calculations had several sources of uncertainty; one of the most important was the contribution of the $a_0(980)$ resonance, for which not even the sign was known. Thus, one is led to rely directly on mechanisms for the reaction, leaving aside the strict chiral counting.

The theoretical situation improved significantly with the thorough revision of the problem in [8], where the different sources of uncertainty were studied and the $a_0(980)$ contribution was reliably included by using the unitary extensions of ChPT [15–18]. Within this chiral unitary approach for the interaction of pseudoscalar mesons, the $a_0(980)$, as well as the $f_0(980)$ or the $\sigma(600)$ resonances, are dynamically generated by using as input the lowest order chiral Lagrangians [19] and resumming the multiple scattering series by means of the Bethe-Salpeter equation. Another source of corrections in [8] was the use of the newest data for radiative decay of vector mesons of the PDG 2002 [2]. It was noted in [8] that the rates had significantly changed from previous editions of the PDG, to the point that the $\eta \rightarrow \pi^0 \gamma \gamma$ widths calculated in [9,14] would have changed by about a factor of 2 should one have used the new data for radiative decay of vector mesons of the PDG 2002 instead of the former ones. Another improvement in [8] was the unitarization of the pair of mesons of the VMD terms beyond the tree level. Furthermore, to have better control of the reaction, the consistency of the model with the related reaction $\gamma \gamma \rightarrow \pi^0 \eta$ was established. Finally, in

[8] a thorough analysis of the theoretical errors was done by considering all sources of uncertainty and making a Monte Carlo sample of results obtained with random values of the input within the uncertainties.

The final result obtained in [8] was

$$\Gamma = 0.42 \pm 0.14 \text{ eV}, \quad (1)$$

which is still in agreement with the present experimental results within uncertainties. Nevertheless, five years after the publication of these results some novelties have appeared that call for a revision of the problem. Indeed, once again the data for the radiative decay of vector mesons of the “online” PDG 2007 [20] have significantly changed with respect to the data of the PDG 2002 used in Ref. [8]. The correction due to these changes is important, and it produces about a 25% decrease in the central value of the result of Eq. (1). At the same time, the theoretical uncertainty is reduced by almost a factor of 2. On the other hand, the new experimental results regarding the two-photon invariant mass distribution [4] provide an extra challenge for the theoretical models.

In view of this, it has become necessary to update the work of [8] to account for the newest experimental results of the PDG 2007 [20] and to compare with the most recent experimental data of the $\eta \rightarrow \pi^0 \gamma \gamma$ decay. The model used here is, hence, the same as the one of [8], and the only change is the use as input of the new radiative widths of the vector mesons. Thus, we refrain from providing detailed explanations on the model, and in this paper we just concentrate on the changes.

II. VMD CONTRIBUTION

Following [9] we consider the VMD mechanism of Fig. 1 which can be easily derived from the VMD

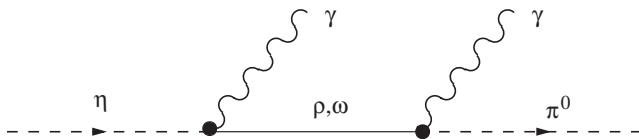


FIG. 1. Diagrams for the VMD mechanism.

Lagrangians involving VVP and $V\gamma$ couplings [21],

$$\begin{aligned} \mathcal{L}_{VVP} &= \frac{G}{\sqrt{2}} \epsilon^{\mu\nu\alpha\beta} \langle \partial_\mu V_\nu \partial_\alpha V_\beta P \rangle, \\ \mathcal{L}_{V\gamma} &= -4f^2 e g A_\mu \langle Q V^\mu \rangle, \end{aligned} \quad (2)$$

where V_μ and P are standard $SU(3)$ matrices for the vector mesons and pseudoscalar mesons, respectively [8]. In Eq. (2) $G = \frac{3g^2}{4\pi^2 f}$, $g = -\frac{G_V M_\rho}{\sqrt{2} f^2}$ [21], and $f = 93 \text{ MeV}$, with G_V the coupling of ρ to $\pi\pi$ in the normalization of [22]. From Eq. (2) one can obtain the radiative decay widths for $V \rightarrow P\gamma$, which are given by

$$\Gamma_{V \rightarrow P\gamma} = \frac{3}{2} \alpha C_i^2 \left(G \frac{2}{3} \frac{G_V}{M_V} \right)^2 k^3, \quad (3)$$

where k is the photon momentum for the vector meson at rest and C_i are $SU(3)$ coefficients that we give in Table I for the different radiative decays, together with the theoretical results (using $G_V = 69 \text{ MeV}$ and $f = 93 \text{ MeV}$) and experimental [2,20] branching ratios. In Table I we quote the results of the PDG 2002 version, which were used as input in the evaluation of the results in [8], together with the new results of the PDG 2007 online edition [20] which are used in the present paper.

The agreement of the theoretical results with the data is fair but it can be improved by incorporating $SU(3)$ breaking mechanisms [23]. For that purpose, we normalize here the C_i couplings so that the branching ratios in Table I agree with experiment.

Once the $VP\gamma$ couplings have been fixed in this way, we can use them in the VMD amplitude corresponding to the diagram of Fig. 1, calculated in detail in [8]. Next we briefly describe the other mechanisms considered in [8].

III. OTHER MECHANISMS

In [8] other mechanisms were considered which are not affected by the modifications of the previous section. We refresh them graphically and refer the reader to [8] for details.

In Fig. 2 we show the diagrams that go through kaon loops. These diagrams, with the unitarization of the

TABLE I. $SU(3)$ C_i coefficients together with theoretical and experimental branching ratios for different vector meson decay processes.

i	C_i	B_i^{th}	B_i^{exp} (PDG 2002 [2])	B_i^{exp} (PDG 2007 [20])
$\rho \rightarrow \pi^0 \gamma$	$\frac{\sqrt{2}}{3}$	7.1×10^{-4}	$(7.9 \pm 2.0) \times 10^{-4}$	$(6.0 \pm 0.8) \times 10^{-4}$
$\rho \rightarrow \eta \gamma$	$\frac{2}{\sqrt{3}}$	5.7×10^{-4}	$(3.8 \pm 0.7) \times 10^{-4}$	$(2.7 \pm 0.4) \times 10^{-4}$
$\omega \rightarrow \pi^0 \gamma$	$\frac{1}{\sqrt{2}}$	12.0%	$8.7 \pm 0.4\%$	$8.91 \pm 0.24\%$
$\omega \rightarrow \eta \gamma$	$\frac{2}{3\sqrt{3}}$	12.9×10^{-4}	$(6.5 \pm 1.1) \times 10^{-4}$	$(4.8 \pm 0.4) \times 10^{-4}$
$K^{*+} \rightarrow K^+ \gamma, K^{*-} \rightarrow K^- \gamma$	$\frac{\sqrt{2}}{3} \left(2 - \frac{M_\omega}{M_\phi} \right)$	13.3×10^{-4}	$(9.9 \pm 0.9) \times 10^{-4}$	$(9.9 \pm 0.9) \times 10^{-4}$
$K^{*0} \rightarrow K^0 \gamma, \bar{K}^{*0} \rightarrow \bar{K}^0 \gamma$	$-\frac{\sqrt{2}}{3} \left(1 + \frac{M_\omega}{M_\phi} \right)$	27.3×10^{-4}	$(23 \pm 2) \times 10^{-4}$	$(23.1 \pm 2.0) \times 10^{-4}$

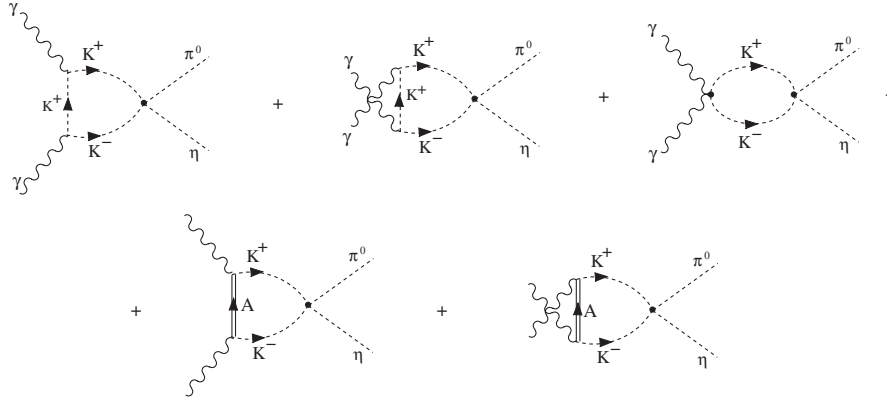


FIG. 2. Diagrams for the chiral loop contribution.

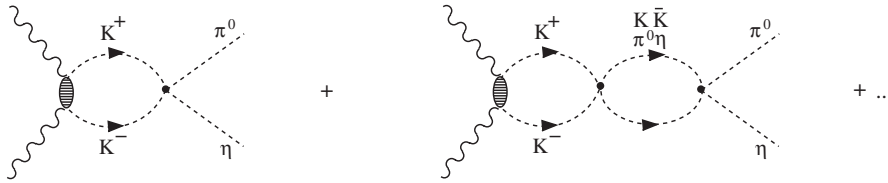


FIG. 3. Resummation for $\gamma \gamma \rightarrow \pi^0 \eta$.

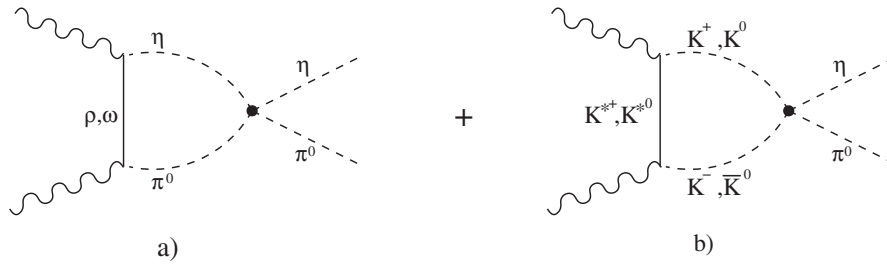


FIG. 4. Loop diagrams for VMD terms. The diagrams with the two crossed photons are not depicted but are also included in the calculations.

meson-meson interaction depicted in Fig. 3, were shown in [24] to be mostly responsible for the strength of the $\gamma \gamma \rightarrow \pi^0 \eta$ reaction in the region of the $a_0(980)$ resonance. It was also shown in [8] that the consideration of the mechanisms of Figs. 1 and 4 improved the agreement with the data at low $\pi^0 \eta$ invariant masses.

The vector meson exchange diagrams of Fig. 1 were unitarized in [8] by including the resummation of diagrams of Fig. 3, producing the diagram depicted in Fig. 4, where

the thick dot represents the full meson-meson unitarized amplitude. Note that these mechanisms are also affected by the renormalization of the VVP vertices discussed in the previous section.

Finally, a small term related to the three-meson axial anomaly, and shown diagrammatically in Fig. 5, was also taken in the calculation since, as noted in [9], although small by itself, it gives a non-negligible contribution upon interference with the other terms.

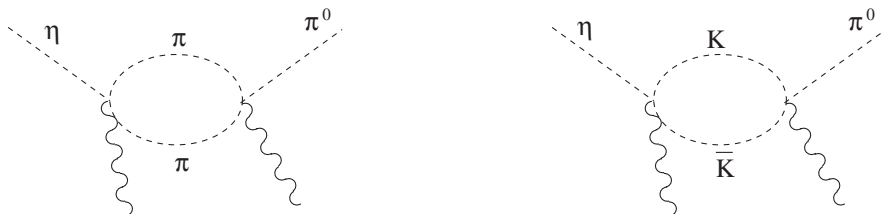


FIG. 5. Diagrams with two anomalous $\gamma \rightarrow 3M$ vertices.

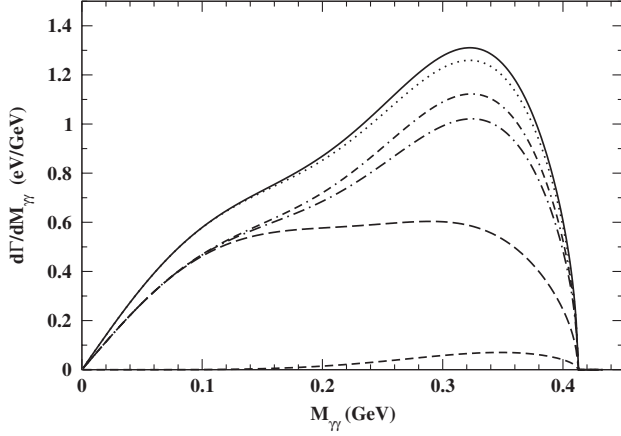


FIG. 6. Contributions to the two-photon invariant mass distribution. From bottom to top, the short-dashed line is for chiral loops, the long-dashed line shows only tree-level VMD, the dashed-dotted line shows the coherent sum of the previous mechanisms, the double dashed-dotted line is the same but with the resummed VMD loops, and the solid line is the same but with the anomalous terms of Fig. 5, which is the full model presented in this work (we are also showing as a dotted line the full model but substituting the full $t_{K^+K^-, \eta\pi^0}$ amplitude by its lowest order).

IV. RESULTS

By considering all the modifications discussed in Sec. II, the integrated width that we obtain is

$$\Gamma = 0.33 \pm 0.08 \text{ eV} \quad (4)$$

which should be compared to the result of [8] of $\Gamma = 0.42 \pm 0.14 \text{ eV}$. The new result compares favorably with the most recent results of Crystal Ball at AGS $\Gamma = 0.285 \pm 0.031 \pm 0.049 \text{ eV}$ and MAMI $\Gamma = 0.290 \pm 0.059 \pm 0.022 \text{ eV}$ [4]. However, all these decay widths are much larger than the preliminary results of KLOE at Frascati $\Gamma = 0.109 \pm 0.035 \pm 0.018 \text{ eV}$ [5].

The mass distribution of the two photons provides extra information which was claimed to be relevant to further test theoretical models. In [8] the differential cross section $d\Gamma/dM_{\gamma\gamma}$ was given. We present here the updated results in Fig. 6, where the contribution of the different mechanisms is shown. The new experiments reported in [4] provide measurements of $d\Gamma/dM_{\gamma\gamma}^2$ which can be contrasted with theoretical predictions.

Note that in the experiments of [4] the magnitude $d\Gamma/dM_{\gamma\gamma}^2$ is given, while in [8] and in Fig. 6 $d\Gamma/dM_{\gamma\gamma}$ is evaluated. Although these distributions are equivalent, in

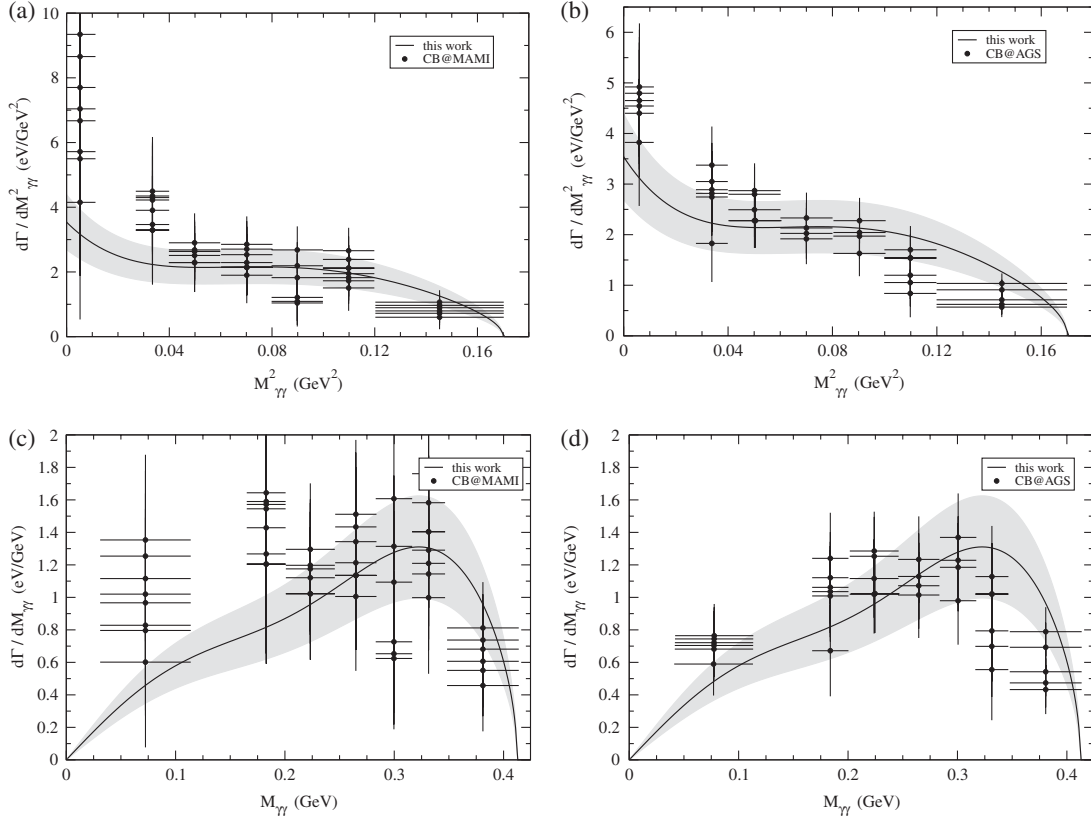


FIG. 7. Two-photon invariant mass squared (upper panels) and two-photon invariant mass (lower panels) distributions. Both the data from Crystal Ball at MAMI (left panels) and those from Crystal Ball at AGS (right panels) are taken from Ref. [4]. The different data in the same bin represent different experimental cuts to filter background sources [4]. The shaded region corresponds to the band of values of the present work considering the theoretical uncertainties.

practice the first one is more useful to study the spectrum at low invariant masses since it provides extra information not given by the second one. Indeed, $d\Gamma/dM_{\gamma\gamma}$ is zero at the threshold of the $\gamma\gamma$ phase space. However, $d\Gamma/dM_{\gamma\gamma}^2$ contains an extra $1/2M_{\gamma\gamma}$ factor and leads to a finite value at zero $\gamma\gamma$ invariant mass. This finite value and the shape of the distribution close to threshold offer an extra test for the theory that would be missed had we simply taken $d\Gamma/dM_{\gamma\gamma}$ for comparison. This of course implies that the measurements can be done with good precision at the threshold. On the other hand, for the high mass region of the spectrum, the $d\Gamma/dM_{\gamma\gamma}$ distribution is more suited to reveal the effects of different theoretical mechanisms, as we have shown in Fig. 6.

In Fig. 7 we compare our theoretical results with the distributions obtained with the Crystal Ball detector at MAMI and AGS. All the experimental data are taken from Ref. [4]. The different experimental points in the same bin represent different cuts implemented in the experimental analysis in order to filter several background sources [4]. This dispersion of the data gives an idea of the uncertainty of the experimental results. The agreement of our results with the experimental data is good, in shape and size, and the theory indeed provides a finite value at threshold compatible with experiment, which nevertheless has large errors. It is interesting to see that the AGS data clearly show an increase of the distribution at low invariant masses, which is a feature of the theoretical results. The data of MAMI, however, have errors that are too large at threshold and do not allow one to see this trend of the results. At large values of the invariant mass the agreement of the theory with MAMI data is better than with AGS data.

In order to offer a different perspective of the comparison of the results at the higher mass region of the distribution, we show in Figs. 7(c) and 7(d) our final results for $d\Gamma/dM_{\gamma\gamma}$ compared to the data of [4] properly transformed to these variables.

V. SUMMARY

In summary, we have witnessed an important experimental advance in recent years on the $\eta \rightarrow \pi^0 \gamma \gamma$ decay. The parallel advances in theory reflected by the work of [8] have allowed a detailed comparison of results, in good agreement both for the total rate and for the invariant mass distributions with the most recent finished results. The discrepancy with the preliminary data of Frascati is worrisome, but we should wait until these data are firm before elaborating further on the discrepancies.

ACKNOWLEDGMENTS

This work is partly supported by DGICYT Contract No. FIS2006-03438, and the Generalitat Valenciana. This research is part of the EU Integrated Infrastructure Initiative HADRON PHYSICS PROJECT under Contract No. RII3-CT-2004-506078. J.R.P.'s research is partially funded by Spanish CICYT Contract No. FPA2007-29115-E, No. FIS2006-03438, No. FPA2005-02327, No. UCM-CAM 910309, as well as Banco Santander/Complutense Contract No. PR27/05-13955-BSCH. L.R. acknowledges further support from Fundación Séneca Grant No. 02975/PI/05 and CICYT Contract No. FPA2004-03470 and No. FPA2007-62777.

-
- [1] D. Aldeet *et al.* *Z. Phys. C* **25**, 225 (1984) [*Yad. Fiz.* **40**, 1447 (1984)]; *Z. Phys. C* **25**, 225 (1984); L. G. Landsberg, *Phys. Rep.* **128**, 301 (1985).
 - [2] K. Hagiwara *et al.* (Particle Data Group Collaboration), *Phys. Rev. D* **66**, 010001 (2002).
 - [3] S. Prakhov *et al.*, *Phys. Rev. C* **72**, 025201 (2005).
 - [4] S. Prakhov, Proceedings of the 11th International Conference on Meson-Nucleon Physics and the Structure of the Nucleon, Juelich, 2007, <http://www.fz-juelich.de/ikp/menu2007/Program/ProgramSessions.shtml>.
 - [5] B. Di Micco *et al.* (KLOE Collaboration), Proceedings of the Eta05 Workshop on Production and Decay of eta and eta-prime Mesons, Cracow, Poland, 2005; *Acta Phys. Slovaca* **56**, 403 (2006).
 - [6] J.N. Ng and D.J. Peters, *Phys. Rev. D* **47**, 4939 (1993).
 - [7] Y. Nemoto, M. Oka, and M. Takizawa, *Phys. Rev. D* **54**, 6777 (1996).
 - [8] E. Oset, J.R. Pelaez, and L. Roca, *Phys. Rev. D* **67**, 073013 (2003).
 - [9] L. Ametller, J. Bijnens, A. Bramon, and F. Cornet, *Phys. Lett. B* **276**, 185 (1992).
 - [10] S. Oneda and G. Oppo, *Phys. Rev.* **160**, 1397 (1968).
 - [11] C. Picciotto, *Nuovo Cimento Soc. Ital. Fis. A* **105**, 27 (1992).
 - [12] A. A. Bel'kov, A. V. Lanyov, and S. Scherer, *J. Phys. G* **22**, 1383 (1996).
 - [13] S. Bellucci and C. Bruno, *Nucl. Phys.* **B452**, 626 (1995).
 - [14] J. Bijnens, A. Fayyazuddin, and J. Prades, *Phys. Lett. B* **379**, 209 (1996).
 - [15] J.A. Oller and E. Oset, *Nucl. Phys.* **A620**, 438 (1997); **A652**, 407(E) (1997).
 - [16] N. Kaiser, *Eur. Phys. J. A* **3**, 307 (1998).
 - [17] J.A. Oller, E. Oset, and J.R. Pelaez, *Phys. Rev. D* **59**, 074001 (1999); **60**, 099906(E) (1999); **75**, 099903(E) (2007).

- [18] J. Nieves and E. Ruiz Arriola, Nucl. Phys. **A679**, 57 (2000).
- [19] S. Weinberg, Phys. Rev. Lett. **18**, 188 (1967).
- [20] W.-M. Yao *et al.* (Particle Data Group), J. Phys. G **33**, 1 (2006) and 2007 partial update for the 2008 edition.
- [21] A. Bramon, A. Grau, and G. Pancheri, Phys. Lett. B **283**, 416 (1992).
- [22] G. Ecker, J. Gasser, A. Pich, and E. de Rafael, Nucl. Phys. **B321**, 311 (1989).
- [23] A. Bramon, A. Grau, and G. Pancheri, Phys. Lett. B **344**, 240 (1995).
- [24] J. A. Oller and E. Oset, Nucl. Phys. **A629**, 739 (1998).